A hydrogen-bonded manganese(II) complex assembled by bipyridyl-organodisulfonate ligands exhibiting ultrahigh superprotonic conductivity

Tao Xu, Ao-Na Sun, Rui-Han Liu, Meng-Tan Cai, Si-Chen Zhang, and Dong Shao *

Hubei Key Laboratory of Processing and Application of Catalytic Materials, Hubei Provincial Engineering Research Center of High Purity Raw Material Processing Technology of Electronic Materials, College of Chemistry and Chemical Engineering, Huanggang Normal University, Huanggang 438000, China.

Correspondence and requests for materials should be addressed to

Email: shaodong@nju.edu.cn

Table of Contents

EXPERIMENTAL SECTION

Materials and Synthesis. All reagents were purchased from commercially available sources and used without further purification. The ligands **H_2bpds** and **22bpy** were bought from TCI chemicals. $Mn(NO_3)_3 \cdot 6H_2O$ was bought from Alfa Aesar.

Synthesis of $[Mn(22bpy)(H_2O)_4]\cdot[22Hbpy]\cdot 1.5[bpds]\cdot 2H_2O$ (MnHOF-102). A mixture was prepared containing $Mn(NO_3)_2 \cdot 6H_2O$ (30 mg, 0.01 mmol), **H_2bpds** (31.4 mg, 0.1 mmol), **22bpy** (15.6 mg, 0.1 mmol), MeCN (2 mL), and water (6 mL). The resulting mixture was stirred for several minutes, and the mixed solution was filtered using a Shimadzu filter. The mixed solution was placed in a 20 ml glass vial and then left to stand for one week. Yellow crystals suitable for X-ray diffraction analysis were obtained in a considerable yield of ca. 59%. Elemental analysis calcd. (%) for $C_{38}H_{41}MnN_4O_{15}S_3$: C, 48.30; H, 4.37; N, 5.92. Found: C, 48.16, H, 4.21; N, 6.07. IR (KBr, cm^{-1}, Figure S10): 3682-2550 (bs), 2831 (s), 1667 (w), 1602 (vs), 1588 (s), 1528 (w), 1473 (s), 1385 (w), 1315 (w), 1201 (vs), 1284(s), 1130 (s),1032 (vs), 997 (vs), 824 (s), 723 (s) cm^{-1}.

Physical measurements

Elemental analyses of C, H, and N were performed at an Elementar Vario MICRO analyzer. Powder X-ray diffraction data (PXRD) were recorded on a Bruker D8 Advance diffractometer with Cu Kα X-ray source (λ = 1.54056 Å) operated at 40 kV and 40 mA. Infrared spectra (IR) data were measured on KBr pellets using a Nexus 870 FT-IR spectrometer in the range of 4000-400 cm^{-1}. Thermal gravimetric analysis (TGA) was measured in Al_2O_3 crucibles using a PerkinElmer Thermal Analysis in the temperature range of 30-700 °C under an Ar atmosphere.

X-ray Crystallography

Single crystal X-ray diffraction data were collected on a Bruker D8 QUEST diffractometer with a PHOTON III area detector (Mo-Kα radiation, λ = 0.71073 Å, Bruker *Ius* 3.0) at 100 K. The APEX III program was used to determine the unit cell parameters and for data collection. The data were integrated and corrected for Lorentz and polarization effects using SAINT.[S1] Absorption corrections were applied with SADABS.[S2] The structures were solved by direct methods and refined by full-matrix least-squares method on *F*2 using the SHELXTL[S3] crystallographic software package integrated in Olex 2.[S4] All the non-hydrogen atoms were refined anisotropically. Hydrogen atoms of the organic ligands were refined as riding on the corresponding non-hydrogen atoms. Additional details of the data collections and structural refinement parameters are provided in Table S1. Selected bond lengths and angles were listed in Table S2 and S3. CCDC 2551344-2551346 are the supplementary crystallographic data for this paper. They can be obtained freely from the Cambridge Crystallographic Data Centre via www.ccdc.cam.ac.uk/data_request/cif.

Proton conductivity

The pellet was prepared by compressing the crystalline powder into a cuboidal shape using a custom-fabricated mold under a pressure of 1000 kg cm^{-2} for 3 min. Alternating current (AC) impedance measurements were performed for a pellet attached to an Au paste with a gold conducting wire using a electrochemical workstation (DH7007). The test cells containing the pellets were suspended in a commercial temperature and humidity control chamber (DHTHM-27-0-P-SD). Data were collected in steps of 10 °C in a frequency range of 0.1 Hz to 10 kHz and an AC amplitude of 100 mV, thermally equilibrated for 2 hours at each temperature. Bulk

conductivities were estimated by a semicircle fitting of Nyquist plots. Proton conductivity (σ) is estimated by the following equation,

$$\sigma = L / A \cdot R \quad (1),$$

where L and A are the thickness and area of the pellet and R is the bulk resistance estimated by the Nyquist plot. Activation energy of proton conduction (E_a) is estimated by the following equation,

$$\sigma T = \sigma_0 \exp (E_a / kBT) \quad (2),$$

where σ is the proton conductivity, σ_0 is the preexponential factor, k_B is the Boltzmann constant, and T is the temperature.

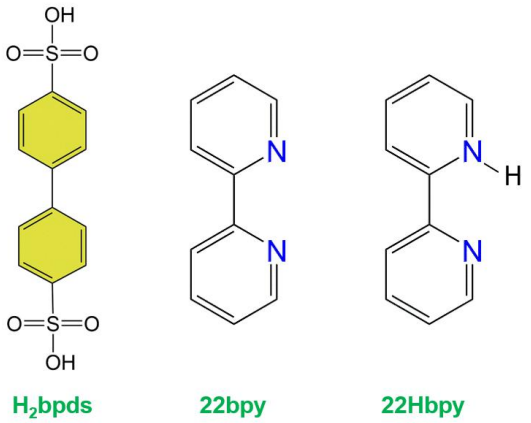

Figure S1. The used organic sulfonic acid and bipyridyl ligand in this work.

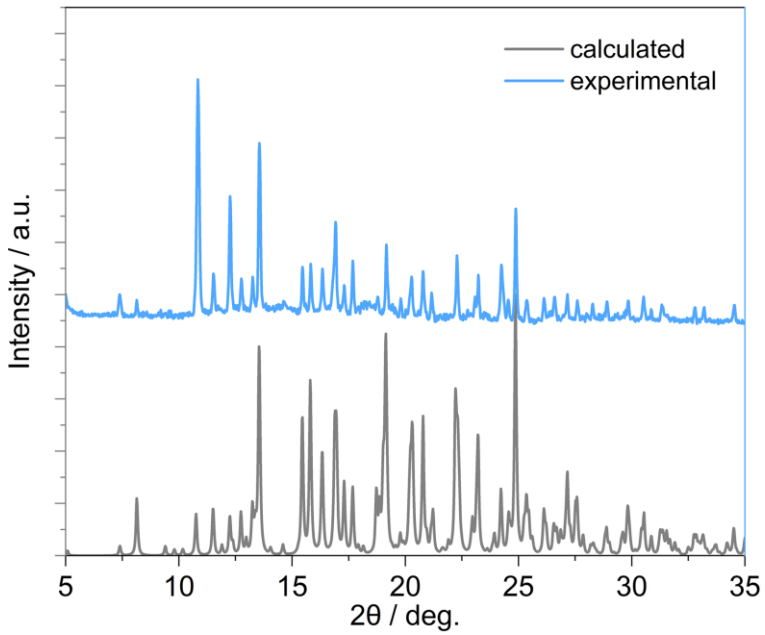

Figure S2. PXRD profiles of as-synthesized **MnHOF-102**.

Table S1. Crystallographic data and structure refinement parameters for **MnHOF-102.**

Temperature / K	293	333	373
Formula		$C_{38}H_{41}MnN_4O_{15}S_3$	
Weight [g mol^{-1}]		944.86	
Crystal system		monoclinic	
Space group		$P2_1/c$	
a [Å]	17.412(4)	17.391(3)	17.360(4)
b [Å]	16.438(5)	16.468(3)	16.507(4)
c [Å]	14.465(4)	14.505(3)	14.562(4)
α [°]	90	90	90
β [°]	93.558(9)	93.998(5)	94.912(8)
γ [°]	90	90	90
V [Å^3]	4132.3(19)	4144.1(12)	4157.9(18)
Z	4	4	4
ρ_{calcd} [g cm^{-3}]	1.517	1.514	1.509
μ(Mo–K_α) [mm^{-1}]	0.546	0.545	0.543
F (000)	1956.0	1960.0	1960.0
R_{int}	0.0858	0.1186	0.1238
R_1 [a] / wR_2 [b] (I > 2σ(I))	0.0478 / 0.1205	0.0608 / 0.1522	0.0948 / 0.2303
R_1/ wR_2 (all data)	0.0718 / 0.1382	0.0956 / 0.1740	0.1161 / 0.2444
GOF on F^2	1.034	1.030	1.063
Max/min [e Å^{-3}]	0.47 / -0.38	0.32 / -0.39	0.48 / -0.36

[a] $R_1 = \sum||F_o| - |F_c||/\sum|F_o|$. [b] $wR_2 = \{\sum[w(F_o^2 - F_c^2)^2]/\sum[w(F_o^2)^2]\}^{1/2}$

Table S2. Selected bond lengths (Å) in **MnHOF-102**.

T / K	293	333	373
Mn1-O1	2.241(2)	2.239(3)	2.232(6)
Mn1-O2	2.162(2)	2.164(4)	2.154(6)
Mn1-O3	2.135(2)	2.139(4)	2.143(7)
Mn1-O4	2.150(2)	2.146(4)	2.183(7)
Mn1-N1	2.247(2)	2.248(3)	2.248(8)
Mn1-N2	2.234(2)	2.245(4)	2.232(8)

Table S3. Selected bond angles (˚) in **MnHOF-102**.

T / K	293	333	373
O1-Mn1-N1	94.86(10)	94.60(14)	95.2(2)
O4-Mn1-O1	90.07(11)	90.04(14)	84.5(3)
O4-Mn1-O2	97.93(14)	98.30(19)	97.8(3)
O4-Mn1-N1	167.83(13)	167.97(18)	167.1(3)
O4-Mn1-N2	95.75(13)	95.43(17)	94.9(3)
O2-Mn1-O1	84.26(12)	84.42(15)	89.4(2)
O2-Mn1-N1	93.63(12)	93.20(17)	94.4(3)
O2-Mn1-N2	165.53(13)	165.60(17)	166.8(3)
O3-Mn1-O1	176.45(10)	176.13(14)	172.8(3)
O3-Mn1-O4	87.21(13)	87.12(18)	89.2(3)
O3-Mn1-O2	93.84(15)	93.4(2)	88.1(3)
O3-Mn1-N1	88.25(12)	88.70(16)	88.8(3)
O3-Mn1-N2	91.49(13)	91.60(18)	95.5(3)

Table S4. Continuous Shape Measure analysis for Mn^{II} centers in **MnHOF-102.**

Metal center	Parameters	CShM value			Coordination geometry
		293 K	333 K	373 K	
Mn^{II}	HP-6	31.561	31.654	31.730	OC-6
	PPY-6	25.250	25.456	24.492	
	OC-6	**0.921**	**0.900**	**1.027**	
	TPR-6	12.538	12.508	11.855	
	JPPY-6	29.146	29.358	28.257	

*CShM [S5] parameters for six-coordinated complexes:

HP-6 - the parameter related to the hexagon (D_{6h})

PPY-6 - the parameter related to the pentagonal pyramid (C_{5v})

OC-6 - the parameter related to the octahedron (O_h)

TPR-6 - the parameter related to the trigonal prism (D_{3h})

JPPY-6 - the parameter related to the Johnson pentagonal pyramid (*C5v*)

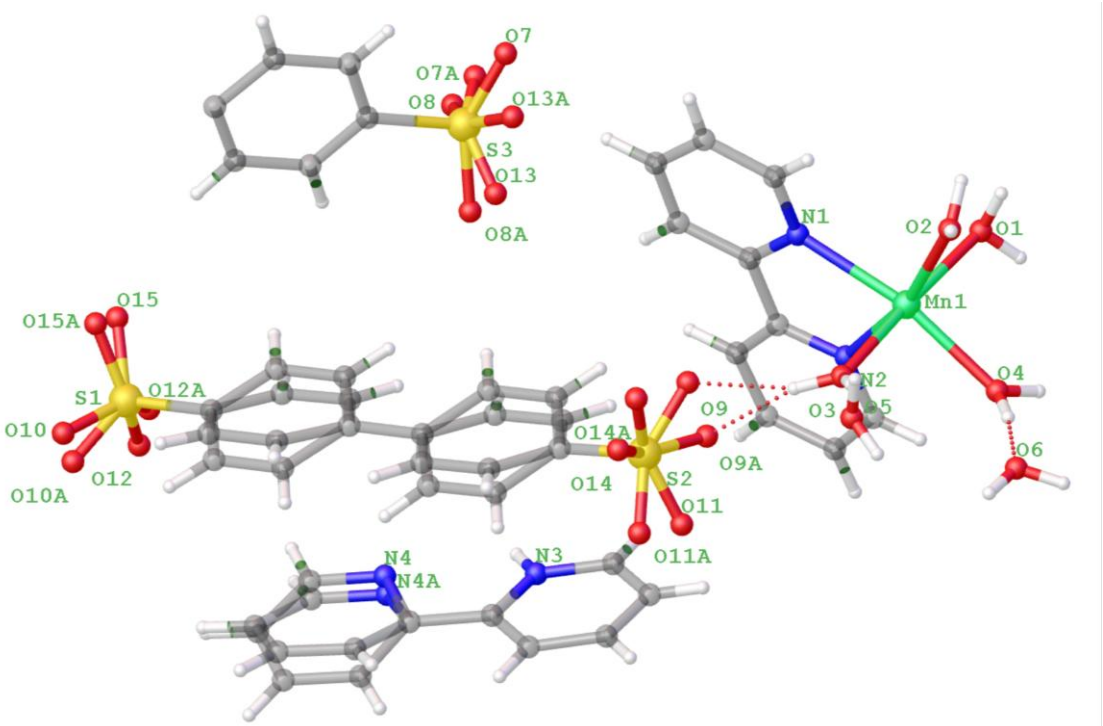

Figure S3. The asymmetric unit of **MnHOF-102** at 293 K.

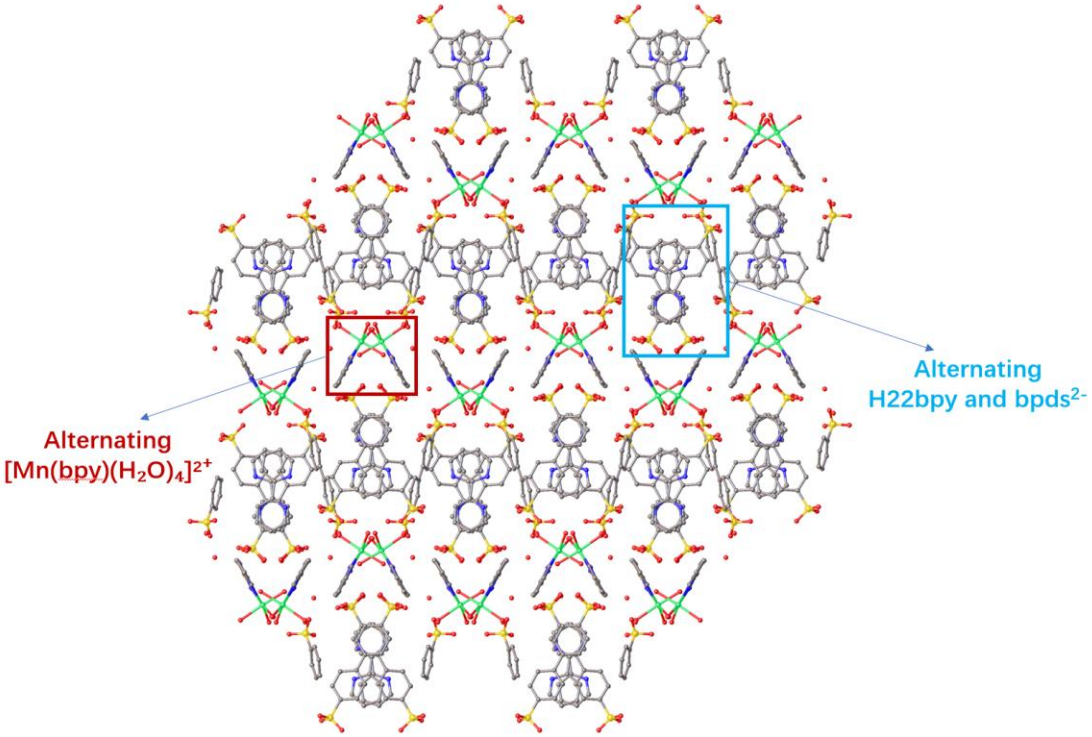

Figure S4. Portion of packing structure of **MnHOF-102**.

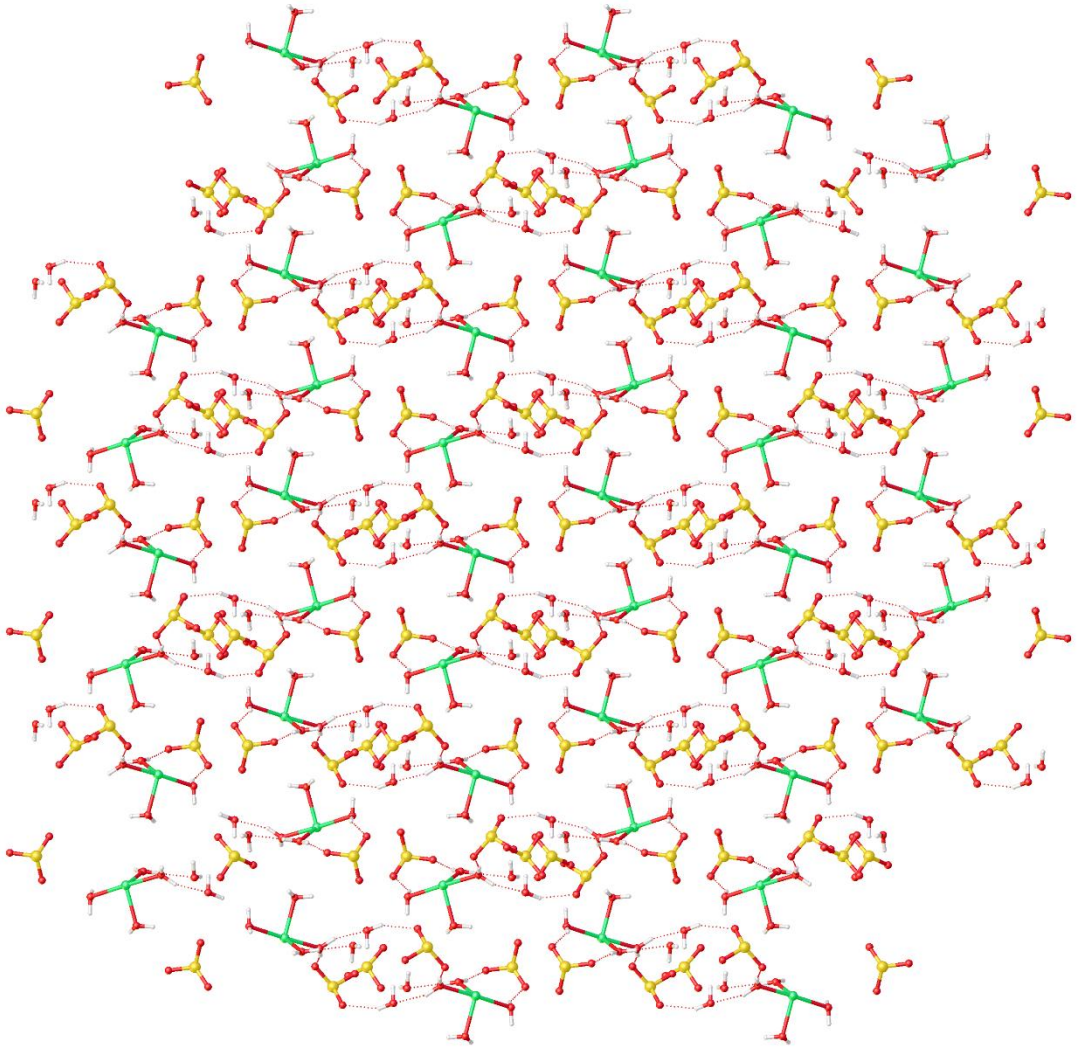

Figure S5. Hydrogen-bonded network in **MnHOF-102** without the indication of C and N atoms along *a* axis.

Table S5. The possible hydrogen bonds in **MnHOF-102** at 293 K calculated by PLATON.

D-H...A	d(D- H)	d(H...A)	d(D...A)	< (DHA)
O1-H(1A) ..O(13)	0.85	1.93	2.7175	152
O1-H(1B) ..O(10)	0.85	2.56	3.3206	149
O1-H(1B) ..O(12)	0.85	2.29	2.9943	140
O2-H(2A) ..O(10)	0.86	2.43	2.737	102
O2-H(2B) ..O(8)	0.86	2.47	2.9043	112
N3-H(3) ..N(4)	0.78	2.34	2.6662	106
N3-H(3) ..O(15)	0.78	2.51	3.1165	136
O3-H(3A) ..O(5)	0.85	1.77	2.5988	164
O3-H(3B) ..O(9)	0.85	1.87	2.6927	164
O4-H(4A) ..O(6)	0.85	1.84	2.6836	170
O4-H(4B) ..O(8)	0.85	1.92	2.7522	168
O5-H(5B) ..O(11)	0.85	1.96	2.7149	147
O6-H(6B) ..O(10)	0.85	2.37	2.9518	126
O6-H(6B) ..O(15)	0.85	2.43	3.2817	175

Table S6. The possible hydrogen bonds in **MnHOF-102** at 333 K calculated by PLATON.

D-H...A	d(D- H)	d(H...A)	d(D...A)	< (DHA)
O1-H(1A) ..O(7)	0.86	1.98	2.7353	146
O1-H(1B) ..O(10)	0.86	2.57	3.3493	152
O1-H(1B) ..O(12)	0.86	2.26	2.9885	143
O2-H(2A) ..O(10)	0.86	2.34	2.728	108
O2-H(2B) ..O(9)	0.86	2.52	2.9232	110
N3-H(3A) ..O(5)	0.85	1.77	2.5714	156
N3-H(3B) ..O(8)	0.85	1.84	2.6812	168
O3-H(3C) ..N(4)	0.86	2.28	2.663	107

O3-H(3C) ..O(15)	0.86	2.46	3.0979	131
O4-H(4A) ..O(6)	0.85	1.91	2.7057	155
O4-H(4B) ..O(9)	0.85	1.92	2.7585	171
O5-H(5A) ..O(3)	0.85	2.14	2.5714	111
O5-H(5B) ..O(11)	0.85	2.02	2.7069	137
O6-H(6A) ..O(4)	0.85	1.98	2.7057	142

Table S7. The possible hydrogen bonds in **MnHOF-102** at 373 K calculated by PLATON.

D-H...A	d(D- H)	d(H...A)	d(D...A)	< (DHA)
O1-H(1A) ..O(8)	0.85	1.93	2.7756	175
O1-H(1B) ..O(12)	0.85	2.11	2.9503	169
O2-H(2A) ..O(6)	0.85	1.92	2.7034	153
O2-H(2B) ..O(10)	0.85	1.96	2.775	161
O3-H(3A) ..O(9)	0.97	1.69	2.6264	159
N3-H(3C) ..N(4)	0.86	2.28	2.6638	107
N3-H(3C) ..O(7)	0.86	2.36	3.02	134
O4-H(4A) ..O(15)	0.86	1.89	2.733	167
O4-H(4B) ..O(10)	0.86	2.41	2.9103	117
O5-H(5A) ..O(13)	0.85	2.38	2.7218	104
O5-H(5A) ..O(6)	0.85	2.48	3.0908	130
O5-H(5B) ..O(3)	0.85	1.66	2.4056	144
O6-H(6A) ..O(2)	0.85	2.35	2.7034	106
O6-H(6B) ..O(15)	0.85	2.16	2.9218	149

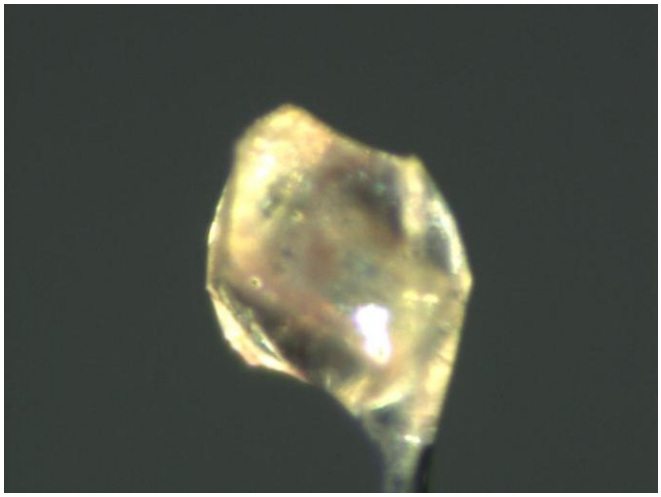

Figure S6. Photograph of a single crystal in **MnHOF-102** at 373 K.

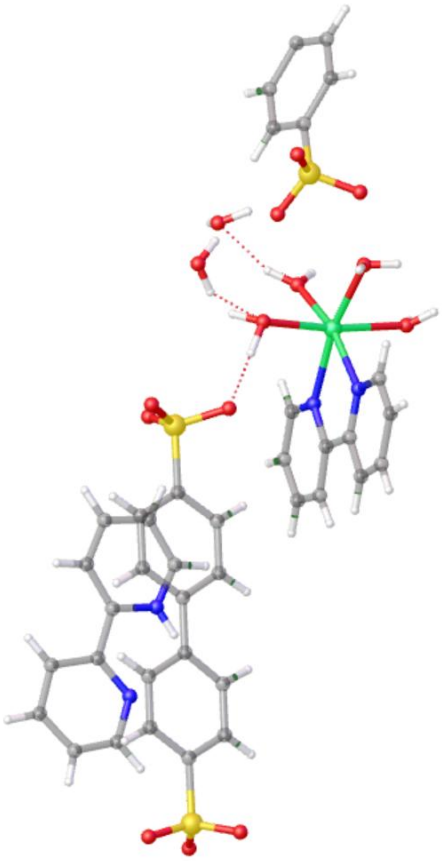

Figure S7. The asymmetric unit of **MnHOF-102** at 373 K.

Table S8. The conductivity of **MnHOF-102** extracted from impedance spectra gathered at 40 °C under variable relative humidity.

RH %	σ / S cm^{-1}
45	7.11×10^{-7}
55	1.73×10^{-7}
65	7.73×10^{-6}
75	1.26×10^{-6}
85	2.61×10^{-5}
95	3.12×10^{-4}

Table S9. The conductivity of **MnHOF-102** extracted from impedance spectra gathered at different temperature under 95% relative humidity.

T / °C	σ / S cm^{-1}
30	6.03×10^{-5}
40	2.02×10^{-4}
50	2.41×10^{-4}
60	3.45×10^{-4}
70	4.42×10^{-4}
80	5.52×10^{-3}
90	1.08×10^{-2}
100	2.11×10^{-2}

Table S10. Comparison of some proton-conducting materials driven by coordinated water molecules.

Compounds	Conductivity / S cm^{-1}	E_a / eV	Working conditions	Num. of coordinated water	Refs.
{[Co(bpy)(H_2O)$_2$(NO_3)$_2$]·H_2O}$_n$	2.99 × 10^{-1}	0.17	85 °C; 95 %	2	S6
{[Co(bpy)(H_2O)$_4$](Hbtc)·(H_2O)$_{1.5}$}$_n$	1.49 × 10^{-1}	0.4	80 °C; 98 %	4	S7
{[Co(bpy)(H_2O)$_4$](btec)$_{0.5}$·H_2O}$_n$	4.15 × 10^{-2}	0.29	80 °C; 98 %	2	S7
[Mn(22bpy)(H_2O)$_4$]·[22Hbpy]·1.5bpds·2H_2O	**2.11 × 10^{-2}**	**0.38**	**100 °C; 95%**	**4**	**This work**
{[Co(bpy)(H_2O)$_4$](fdc)·(H_2O)$_{1.5}$}$_n$	4.85 × 10^{-3}	0.4	80 °C; 98 %	5	S7
{[Mg_2(OBA)$_2$(H_2O)$_6$]·2H_2O}$_n$	1.27 × 10^{-2}	0.13	80 °C; 95 %	6	S8
{[Tb_4(TTHA)$_2$(H_2O)$_4$]·7H_2O}$_n$	2.57× 10^{-2}	0.68	60 °C; 98 %	4	S9
{[Co(bpy)$_3$(H_2O)$_2$](bpy)·2NO_3· (5.4H_2O)}$_n$	1.85 × 10^{-2}	0.38	80 °C; 98 %	2	S10
[Fe($C_6N_6O_2$)(H_2O)$_4$]·5H_2O	2.1 × 10^{-3}	0.68	22 °C; 95 %	4	S11
[Co(H_2O)$_6$][H_2tcba]	1.6 × 10^{-3}	0.31	100 °C; 97 %	6	S12
Fe(ox)·2H_2O	1.3 × 10^{-3}	0.37	25 °C; 98 %	2	S13
[Co_2(dobdc)(H_2O)$_2$]·6H_2O	6.1× 10^{-4}	0.15	90 °C; 95 %	2	S14
{[Cu_4(μ$_3$-OH)4(4,4'-bpy)$_2$(2,6-NDS)(H_2O)$_7$]·2,6NDS·6H2O}$_n$	5.2 × 10^{-4}	0.78	80 °C; 98 %		S15
[Co(QLC)$_2$·(H_2O)$_2$]	1.4 × 10^{-4}	0.39	70 °C; 97 %	2	S16
[Mg_2(dstp)(H_2O)$_4$]·3H_2O·0.5DEF	1.3× 10^{-4}	0.19	80 °C; 50 %	4	S17
[Ca_2(BTC)(DMA)(H_2O)]	2.0 × 10^{-5}	0.40	25 °C; 98 %	1	S18
[Cu_3(BTC)$_2$(H_2O)$_3$]$_n$	1.5 × 10^{-5}	/	25 °C	3	S19

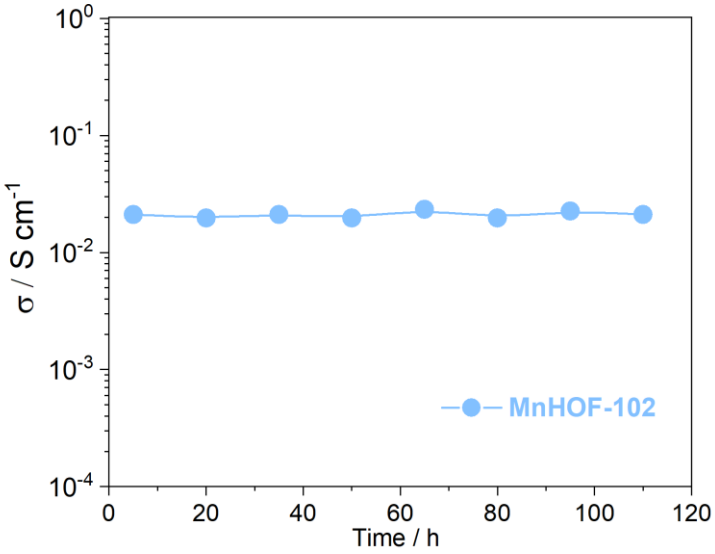

Figure 8. Time-dependent proton conductivity of **MnHOF-102** at 100 °C and 95% RH.

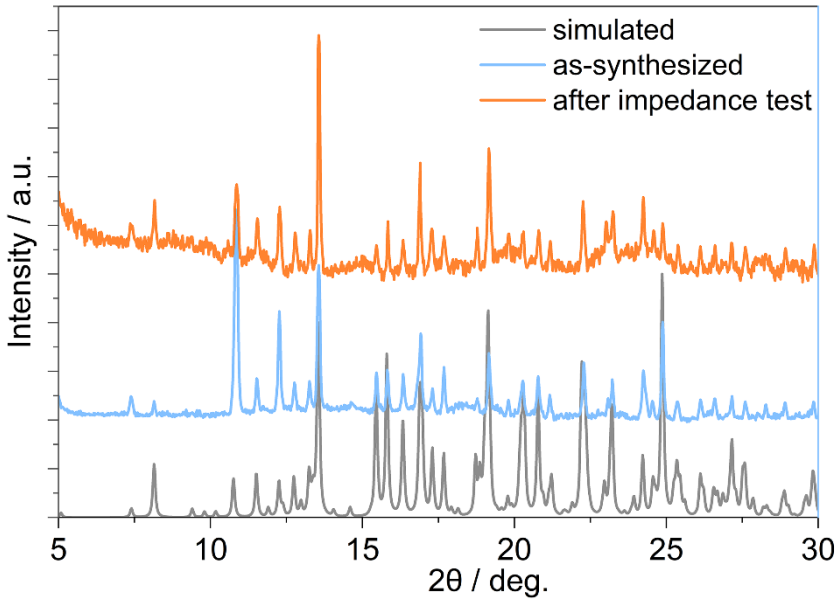

Figure 9. PXRD spectra before and after impedance measurements for **MnHOF-102**.

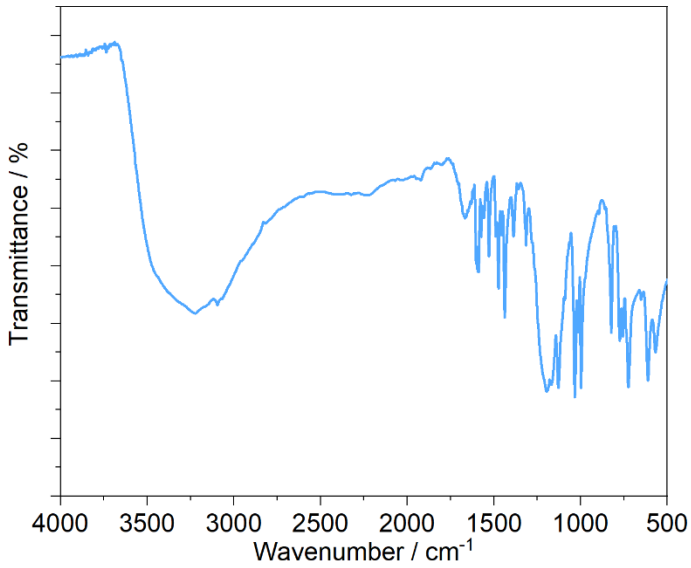

Figure S10. Infrared spectra of **MnHOF-102**.

References

1) SAINT Software Users Guide, version 7.0; Bruker Analytical X-Ray Systems: Madison, WI, 1999.

2) G. M. Sheldrick, SADABS, version 2.03; Bruker Analytical X-Ray Systems, Madison, WI, 2000.

3) G. M. Sheldrick, SHELXTL, Version 6.14, Bruker AXS, Inc.; Madison, WI 2000-2003.

4) Dolomanov, O. V.; Bourhis, L. J.; Gildea, R. J.; Howard, J. A. K.; Puschmann, H. OLEX2: A Complete Structure Solution, Refinement and Analysis Program. *J. Appl. Crystallogr.*, 2009, 42, 339−341.

5) M. Llunell, D. Casanova, J. Cirera, P. Alemany and S. Alvarez, SHAPE, Version 2.1. Universitat de Barcelona, 2013.

6) S. C. Pal, D. Mukherjee, Y. Oruganti, B. G. Lee, D.-W. Lim, B. Pramanik, A. K. Manna and M. C. Das, J. Am. Chem. Soc., 2024, 146, 14546–14557.

7) S. M. Elahi, S. Chand, W.-H. Deng, A. Pal and M. C. Das, Angew. Chem. Int. Ed., 2018, 57, 6662–6666.

8) S. Chand, S. C. Pal, D.-W. Lim, K. Otsubo, A. Pal, H. Kitagawa and M. C. Das, ACS Mater. Lett., 2020, 2, 1343–1350.

9) L. Feng, H.-S. Wang, H.-L. Xu, W.-T. Huang, T.-Y. Zeng, Q.-R. Cheng, Z.-Q. Pan and H. Zhou, Chem. Commun., 2019, 55, 1762–1765.

10) S. C. Pal, S. Chand, A. G. Kumar, P. G. M. Mileo, I. Silverwood, G. Maurin, S. Banerjee, S. M. Elahi and M. C. Das, J. Mater. Chem. A, 2020, 8, 7847–7853.

11) H. Bunzen, A. Javed, D. Klawinski, A. Lamp, M. Grzywa, A. Kalytta-Mewes, M. Tiemann, H.-A. K. von Nidda, T. Wagner and D. Volkmer, ACS Appl. Nano Mater., 2019, 2, 291–298.

12) D. Shao, Y. Zhou, X. Yang, J. Yue, S. Ming, X.-Q. Wei and Z. Tian, Dalton Trans., 2022, 51, 18514–18519.

13) T. Yamada, M. Sadakiyo and H. Kitagawa, J. Am. Chem. Soc., 2009, 131, 3144–3145.

14) S. Hwang, E. J. Lee, D. Song and N. C. Jeong, ACS Appl. Mater. Interfaces, 2018, 10, 35354–35360.

15) R. Sahoo, S. Luo, N. K. Pendyala, S. Chand, Z.-H. Fu and M. C. Das, Mater. Chem. Front., 2023, 7, 3373–3381.

16) X.-M. Bu, S.-Y. Yang, Q. Zhang, L.-Z. Han, E.-S. Xiang, X.-C. Huang, L. Shi and D. Shao, J. Mol. Struct., 2023, 1286, 135544.

17) J. H. Lee, H. Kim, M. Kang, D. S. Choi and C. S. Hong, Bull. Korean Chem. Soc., 2021, 42, 322–325.

18) A. Mallick, T. Kundu and R. Banerjee, Chem. Commun., 2012, 48, 8829–8831.

19) N. C. Jeong, B. Samanta, C. Y. Lee, O. K. Farha and J. T. Hupp, J. Am. Chem. Soc., 2012, 134, 51–54.